



Search for the doubly charmed baryon Ω_{cc}^+

LHCb collaboration[†]

Abstract

A search for the doubly charmed baryon Ω_{cc}^+ with the decay mode $\Omega_{cc}^+ \rightarrow \Xi_c^+ K^- \pi^+$ is performed using proton-proton collision data at a centre-of-mass energy of 13 TeV collected by the LHCb experiment from 2016 to 2018, corresponding to an integrated luminosity of 5.4 fb^{-1} . No significant signal is observed within the invariant mass range of 3.6 to 4.0 GeV/c^2 . Upper limits are set on the ratio R of the production cross-section times the total branching fraction of the $\Omega_{cc}^+ \rightarrow \Xi_c^+ K^- \pi^+$ decay with respect to the $\Xi_{cc}^{++} \rightarrow \Lambda_c^+ K^- \pi^+ \pi^+$ decay. Upper limits at 95% credibility level for R in the range 0.005 to 0.11 are obtained for different hypotheses on the Ω_{cc}^+ mass and lifetime in the rapidity range from 2.0 to 4.5 and transverse momentum range from 4 to 15 GeV/c .

Published in Sci. China-Phys. Mech. Astron. 64, 101062 (2021)

© 2021 CERN for the benefit of the LHCb collaboration. CC BY 4.0 licence.

[†]Authors are listed at the end of this paper.

1 Introduction

The quark model [1–3] predicts the existence of multiplets of baryon states with a structure containing three valence quarks, two charm quarks and a light quark (u , d or s). There are three doubly charmed, weakly decaying states expected: a Ξ_{cc} isodoublet (ccu , ccd) and an Ω_{cc}^+ isosinglet (ccs), each with spin-parity $J^P = 1/2^+$. Theoretical models [4–7] predict that the light quark moves with a large relative velocity with respect to the bound (cc)-diquark inside the baryon and experiences a short-range of QCD potential.

The Ξ_{cc}^{++} baryon with mass $3620.6 \pm 1.6 \text{ MeV}/c^2$ was first observed by the LHCb collaboration in the $\Lambda_c^+ K^- \pi^+ \pi^+$ decay¹ [8], and confirmed in the $\Xi_c^+ \pi^+$ decay [9]. The search for Ξ_{cc}^+ via its decay to $\Lambda_c^+ K^- \pi^+$ was updated recently by the LHCb collaboration, and no significant signal was found [10]. The Ω_{cc}^+ mass is predicted to be in the range $3.6 - 3.9 \text{ GeV}/c^2$ [6, 11–20] and its lifetime is predicted to be $75 - 180 \text{ fs}$ [6, 21–26]. Due to destructive Pauli interference [21], the Ξ_{cc}^{++} and Ω_{cc}^+ baryons have a larger lifetime than that of the Ξ_{cc}^+ baryon which is shortened by the contribution from W boson exchange between the charm and down quarks. In proton-proton (pp) collisions at a centre-of-mass energy of 13 TeV, the production cross-section of the doubly charmed baryons is predicted to be within the range of $60 - 1800 \text{ nb}$ [5, 7, 26–30], which is between 10^{-4} and 10^{-3} times that of the total charm quark production [31]. The production cross-section of the Ω_{cc}^+ baryon is expected to be about 1/3 of those of the Ξ_{cc}^+ and Ξ_{cc}^{++} baryons due to the presence of an s quark [32]. A discovery of the Ω_{cc}^+ baryon and measurements of its properties would validate the aforementioned theoretical predictions, and deepen our understanding on the dynamics in the production and decays of the doubly charmed baryons.

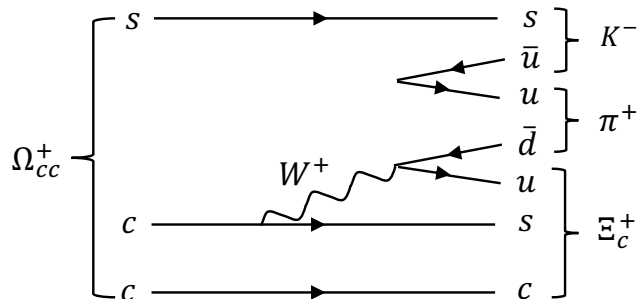


Figure 1: Example Feynman diagram for the $\Omega_{cc}^+ \rightarrow \Xi_{cc}^+ K^- \pi^+$ decay.

In this paper, a search for the Ω_{cc}^+ baryon via the $\Omega_{cc}^+ \rightarrow \Xi_{cc}^+ K^- \pi^+$ decay, which is predicted to have a relatively large branching fraction [33, 34], is presented. The data are collected by the LHCb experiment in pp collisions at a centre-of-mass energy of 13 TeV in the period from 2016 to 2018. A possible Feynman diagram for this decay is shown in Fig. 1.

In order to avoid experimenters’ bias, the results of the analysis were not examined until the full procedure had been finalised. Two different selections are developed: selection A is optimised to maximise the hypothetical signal sensitivity and selection B is optimised for the production ratio measurement. The analysis strategy is defined as follows: selection A is first used to search for Ω_{cc}^+ signal and evaluate its significance as a function of Ω_{cc}^+

¹Inclusion of charge-conjugated processes is implied throughout this paper.

mass. If evidence for a signal with a global significance above 3 standard deviations after considering the look-elsewhere effect would be found, the mass would be measured and Selection B would be employed to measure the production cross-section of the Ω_{cc}^+ baryon; else, upper limits on the production ratio R as a function of the Ω_{cc}^+ mass for different lifetime hypotheses would be set. The production ratio R , relative to the $\Xi_{cc}^{++} \rightarrow \Lambda_c^+ K^- \pi^+ \pi^+$ decay, is defined as

$$R \equiv \frac{\sigma(\Omega_{cc}^+) \times \mathcal{B}(\Omega_{cc}^+ \rightarrow \Xi_c^+ K^- \pi^+) \times \mathcal{B}(\Xi_c^+ \rightarrow p K^- \pi^+)}{\sigma(\Xi_{cc}^{++}) \times \mathcal{B}(\Xi_{cc}^{++} \rightarrow \Lambda_c^+ K^- \pi^+ \pi^+) \times \mathcal{B}(\Lambda_c^+ \rightarrow p K^- \pi^+)}, \quad (1)$$

where σ is the baryon production cross-section and \mathcal{B} is the branching fraction of the corresponding decays. Both the Ω_{cc}^+ and Ξ_{cc}^{++} baryons are required to be in the rapidity range of 2.0 to 4.5 and have transverse momentum between 4 and 15 GeV/ c .

The production ratio is evaluated as

$$R = \frac{\varepsilon_{\text{norm}}}{\varepsilon_{\text{sig}}} \frac{N_{\text{sig}}}{N_{\text{norm}}} \equiv \alpha N_{\text{sig}}, \quad (2)$$

where ε_{sig} and $\varepsilon_{\text{norm}}$ refer to the efficiencies of the Ω_{cc}^+ signal and the Ξ_{cc}^{++} normalisation decay mode, respectively, N_{sig} and N_{norm} are the corresponding yields, and α is the single-event sensitivity. The lifetime of the Ω_{cc}^+ baryon is unknown and strongly affects the selection efficiency, hence upper limits on R are quoted as a function of the Ω_{cc}^+ baryon mass for a discrete set of lifetime hypotheses.

2 Detector and simulation

The LHCb detector [35, 36] is a single-arm forward spectrometer covering the pseudorapidity range $2 < \eta < 5$, designed for the study of particles containing b or c quarks. The detector includes a high-precision tracking system consisting of a silicon-strip vertex detector surrounding the pp interaction region [37], a large-area silicon-strip detector located upstream of a dipole magnet with a bending power of about 4 Tm, and three stations of silicon-strip detectors and straw drift tubes [38, 39] placed downstream of the magnet. The tracking system provides a measurement of the momentum, p , of charged particles with a relative uncertainty that varies from 0.5% at low momentum to 1.0% at 200 GeV/ c . The minimum distance of a track to a primary pp -collision vertex (PV), the impact parameter (IP), is measured with a resolution of $(15 + 29/p_T) \mu\text{m}$, where p_T is the component of the momentum transverse to the beam, in GeV/ c . Different types of charged hadrons are distinguished using information from two ring-imaging Cherenkov detectors [40]. The online event selection is performed by a trigger [41], which consists of a hardware stage, based on information from the calorimeter and muon systems, followed by a software stage, which applies a full event reconstruction.

Simulated samples are required to develop the event selection and to estimate the detector acceptance and the efficiency of the imposed selection requirements. Simulated pp collisions are generated using PYTHIA [42] with a specific LHCb configuration [43]. A dedicated generator, GENXICC2.0 [44], is used to simulate the doubly charmed baryon production. Decays of unstable particles are described by EVTGEN [45], in which final-state radiation is generated using PHOTOS [46]. The interaction of the generated particles with the detector, and its response, are implemented using the GEANT4 toolkit [47] as

described in Ref. [48]. The $\Omega_{cc}^+ \rightarrow \Xi_c^+ K^- \pi^+$ decay is assumed to proceed according to a uniform phase-space model. The Ω_{cc}^+ baryon and Ξ_{cc}^{++} baryon are assumed to have no polarization. Unless otherwise stated, simulated events are generated with an Ω_{cc}^+ (Ξ_{cc}^{++}) mass of $3738 \text{ MeV}/c^2$ ($3621 \text{ MeV}/c^2$) and a lifetime of 160 fs (256 fs).

3 Reconstruction and selection

The Ω_{cc}^+ signal mode is reconstructed by combining a Ξ_c^+ candidate with kaon and pion candidates coming from the same vertex. The Ξ_c^+ candidates are firstly formed by combining three tracks originating from the same vertex, displaced with respect to the PV; at least one track is required to satisfy an inclusive software trigger based on a multivariate classifier [49, 50], and the three tracks must satisfy particle identification (PID) requirements to be compatible with a $pK^-\pi^+$ hypothesis. Then the Ξ_c^+ candidates with good vertex quality and invariant mass within the region of 2450 to 2486 MeV/c^2 are combined with two extra tracks, identified as K^- and π^+ , to reconstruct a Ω_{cc}^+ candidate. The Ξ_c^+ mass region is defined as $2468 \pm 18 \text{ MeV}/c^2$ where the mean value is the known Ξ_c^+ mass [51] and the width is corresponding to three times the mass resolution.

To improve further the Ω_{cc}^+ signal purity, a multivariate classifier based on a boosted decision tree (BDT) [52, 53] is developed to suppress combinatorial background. The classifier is trained using simulated Ω_{cc}^+ events as signal and wrong-sign $\Xi_c^+ K^- \pi^-$ combinations in data with mass in the interval 3600 to 4000 MeV/c^2 to represent background.

For selection A, no specific trigger requirement is applied. A multivariate selection is trained with two sets of variables which show good discrimination between Ω_{cc}^+ signal and background. The first set contains variables related to the reconstructed Ω_{cc}^+ candidates, including the Ω_{cc}^+ decay vertex-fit quality, such as χ_{IP}^2 , the pointing angle and the flight-distance χ^2 . Here χ_{IP}^2 is the difference in χ^2 of the PV reconstructed with and without the Ω_{cc}^+ candidate, the pointing angle is the three-dimensional angle between the Ω_{cc}^+ candidate momentum direction and the vector joining the PV and the reconstructed Ω_{cc}^+ decay vertex, while the flight-distance χ^2 is defined as the χ^2 of the hypothesis that the decay vertex of the candidate coincides with its associated PV. The second set adds variables related to the decay products (p , K^- and π^+ from the Ξ_c^+ decay, and K^- and π^+ from the Ω_{cc}^+ decay), including momentum, transverse momentum, χ_{IP}^2 and PID variables.

The threshold of the multivariate output is determined by maximising the figure of merit $\varepsilon / (5/2 + \sqrt{N_B})$ [54], where ε is the estimated MVA selection efficiency, 5/2 corresponds to 5 standard deviations in a Gaussian significance test, and N_B is the expected number of background candidates in the signal region, estimated with the wrong-sign $\Xi_c^+ K^- \pi^-$ combinations in the mass region of $\pm 12.5 \text{ MeV}/c^2$ around the Ω_{cc}^+ mass of $3738 \text{ MeV}/c^2$ used in the simulation, taking into account the difference of the background level for the signal sample and the wrong-sign sample.

After the multivariate selection, the reconstructed Ω_{cc}^+ candidates could suffer from background from candidates reconstructed with clone tracks, i.e. reconstructed tracks sharing a large portion of their detector hits. Clone tracks could be included in a Ω_{cc}^+ candidate, when one is used for the π^+ candidate from the Ξ_c^+ decay and its clone for the π^+ candidate from the Ω_{cc}^+ decay. To avoid that, candidates with the angle between each pair of identically charged tracks smaller than 0.5 mrad are removed. The Ω_{cc}^+ candidates could also be formed by the same five final tracks but with two tracks interchanged, *e.g.*

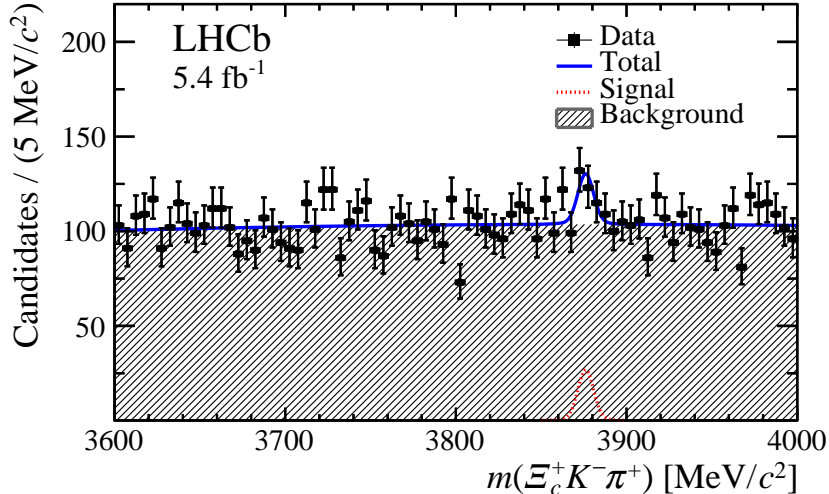


Figure 2: Invariant mass $m(\Xi_c^+ K^- \pi^+)$ distribution of selected Ω_{cc}^+ candidates from (black points) selection A, with (blue solid line) the fit with the largest local significance at the mass of $3876 \text{ MeV}/c^2$ superimposed.

the K^- (π^+) candidate from the Ξ_c^+ decay is swapped with the K^- (π^+) candidate from the Ω_{cc}^+ decay. In this case, only one candidate is chosen randomly.

For selection B, the multivariate selection is similar to selection A except that the PID variables of the K^- and π^+ candidates from the Ω_{cc}^+ decay are not used in the training to ease the efficiency determination. Furthermore, an additional hardware trigger requirement is imposed on candidates for both the signal and the normalisation modes to minimise differences between data and simulation. The data sets are split into two disjoint subsamples. One subsample is triggered on signals associated with one of the reconstructed Ξ_c^+ candidates with high transverse energy deposits in the calorimeters (TOS), and the other is triggered on signals exclusively unrelated to the Ω_{cc}^+ candidate (exTIS).

The reconstruction and selection requirements of the Ξ_{cc}^{++} normalisation mode are similar to those in the Ξ_{cc}^+ search [10,31]. Both Ω_{cc}^+ and Ξ_{cc}^{++} candidates are required to be in the fiducial region of rapidity $2.0 < y < 4.5$ and transverse momentum $4 < p_T < 15 \text{ GeV}/c$.

4 Yield measurements

After applying selection A to the full data sample, the invariant mass distribution $m(\Xi_c^+ K^- \pi^+)$ of selected Ω_{cc}^+ candidates is shown in Fig. 2. To improve the mass resolution, the variable $m(\Xi_c^+ K^- \pi^+)$ is defined as the difference of the reconstructed mass of the Ω_{cc}^+ and Ξ_c^+ candidates plus the known Ξ_c^+ mass [51]. The $m(\Xi_c^+ K^- \pi^+)$ distribution is fitted with a sum of signal and background components, where the signal component is described by the sum of two Crystal Ball functions [55] and the background component by a second-order Chebyshev function. The parameters of the signal shape are fixed from simulation, where the width is found to be around $5.5 \text{ MeV}/c^2$. The parameters of background shape are obtained from a fit to the wrong-sign $\Xi_c^+ K^- \pi^-$ combinations. An unbinned maximum likelihood fit is performed with the peak position varied in steps of

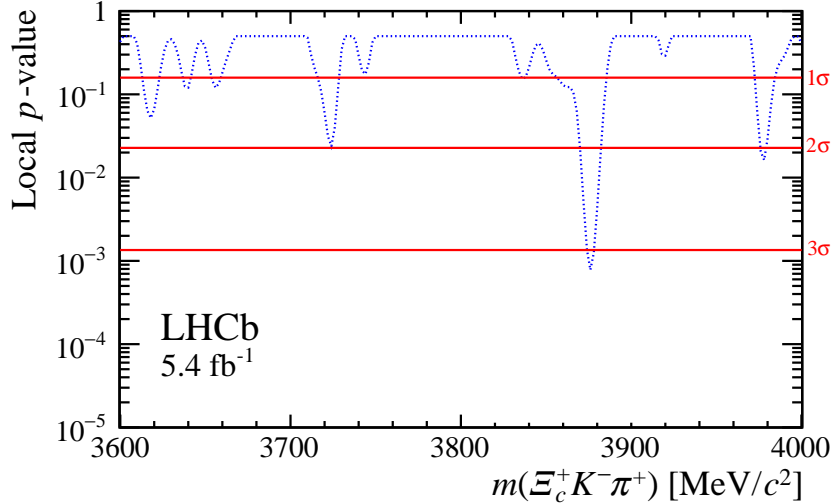


Figure 3: Local p -value at different $m(\Omega_{cc}^+)$ values evaluated with the likelihood ratio test. Lines indicating one, two and three standard deviations (σ) of local significance are also shown.

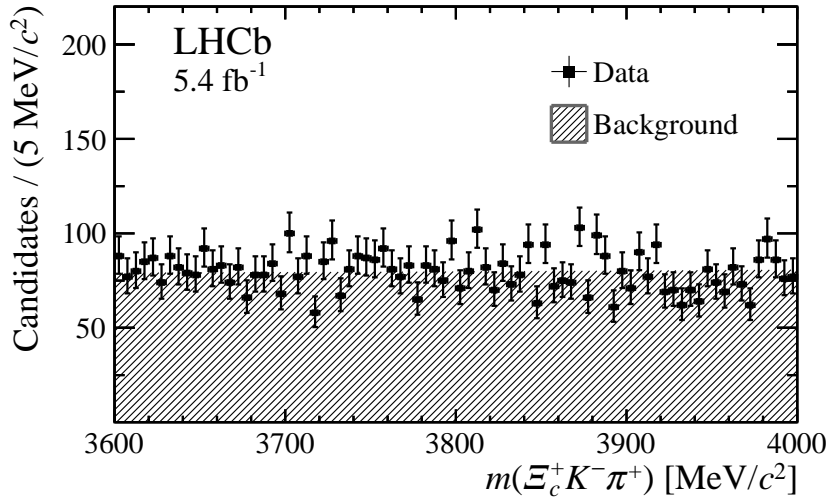


Figure 4: Invariant mass $m(\Xi_c^+ K^- \pi^+)$ distribution of selected Ω_{cc}^+ candidates (black points) with selection B, only background fit is shown.

$2 \text{ MeV}/c^2$, and the largest signal contribution is found for an Ω_{cc}^+ mass of $3876 \text{ MeV}/c^2$.

The local significance of the signal peak is quantified with a p -value, which is calculated as the likelihood ratio of the background plus signal hypothesis and the background-only hypothesis [56, 57]. The local p -value is plotted in Fig. 3 as a function of mass, $m(\Xi_c^+ K^- \pi^+)$, showing a dip around $3876 \text{ MeV}/c^2$, which has the largest local significance, corresponding to 3.2 standard deviations. The global significance is evaluated with pseudoexperiments, by taking into account the look-elsewhere effect [58] in the mass range from $3600 \text{ MeV}/c^2$ to $4000 \text{ MeV}/c^2$, and is estimated to be 1.8 standard deviations. As no excess above 3 standard deviations is observed, upper limits on the production ratios are set by using selection B. The invariant mass distribution of Ω_{cc}^+ candidates is shown in Fig. 4 with the fit under the background-only hypothesis.

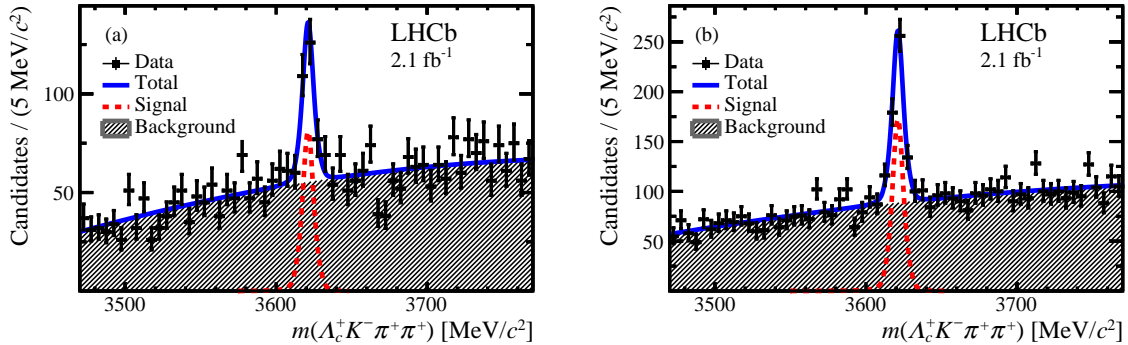


Figure 5: Distribution of invariant mass $m(\Lambda_c^+ K^- \pi^+ \pi^+)$ for selected Ξ_{cc}^{++} candidates in different categories: (a) triggered by one of the Λ_c^+ decay products and (b) triggered exclusively by particles unrelated to the Ξ_{cc}^{++} decay products, in the 2018 data set. The fit results are superimposed.

Table 1: Signal yields for the $\Xi_{cc}^{++} \rightarrow \Lambda_c^+ K^- \pi^+ \pi^+$ normalisation mode N_{norm} for both trigger categories and different data-taking periods with the corresponding integrated luminosity \mathcal{L} . The uncertainties are statistical only.

Year	\mathcal{L} [fb^{-1}]	N_{norm}	
		TOS	extTIS
2016	1.7	126 ± 21	165 ± 23
2017	1.6	145 ± 21	255 ± 26
2018	2.1	164 ± 21	349 ± 30

The measured production ratio is a function of single-event sensitivity α and N_{sig} , as shown in Eq. 2. The parameter α is calculated using the yield of the normalisation mode N_{norm} multiplied by the efficiency ratio between the normalisation and signal modes, while N_{sig} is extracted by fitting the data of the signal mode.

The Ξ_{cc}^{++} yields, N_{norm} , are determined by performing an extended unbinned maximum likelihood fit to the invariant mass in the two trigger categories. The invariant mass distribution $m(\Lambda_c^+ K^- \pi^+ \pi^+)$ is defined as the difference of the reconstructed mass of the Ξ_{cc}^{++} and Λ_c^+ candidates plus the known Λ_c^+ mass [51]. For illustration, the $m(\Lambda_c^+ K^- \pi^+ \pi^+)$ distributions for the 2018 data set are shown in Fig. 5 together with the associated fit projections. The mass shapes of the normalisation mode are a sum of a Gaussian function and a modified Gaussian function with power-law tails on both sides for signal and a second-order Chebyshev polynomial for background, which is the same as used in the Ξ_{cc}^+ search [31]. The Ξ_{cc}^{++} yields are summarised in Table 1, where the TOS refers to the trigger on signal and the extTIS refers to exclusive trigger independently of signal.

5 Efficiency ratio estimation

The efficiency ratio between the Ξ_{cc}^{++} mode and Ω_{cc}^+ mode, defined as $\varepsilon_{\text{norm}}/\varepsilon_{\text{sig}}$, is determined from simulation. The distributions of the transverse momentum, rapidity of the doubly charmed baryons, and the event multiplicity in simulated samples are weighted according to the differences between simulation and data seen for the Ξ_{cc}^{++} baryon. The

Table 2: Efficiency ratios $\varepsilon_{\text{norm}}/\varepsilon_{\text{sig}}$ between normalisation and signal modes for both trigger categories for different data-taking periods, where the TOS refers to the trigger on signal and the exTIS refers to exclusive trigger independently of signal. The uncertainties are statistical only.

Year	$\varepsilon_{\text{norm}}/\varepsilon_{\text{sig}}$	
	TOS	exTIS
2016	0.32 ± 0.03	0.28 ± 0.02
2017	0.55 ± 0.03	0.71 ± 0.02
2018	0.61 ± 0.04	0.69 ± 0.02

Table 3: Single-event sensitivity $\alpha(\Xi_{cc}^{++})$ [10^{-2}] of the Ξ_{cc}^{++} normalisation mode triggered by one of the Ξ_c^+ (Λ_c^+) products for different lifetime hypotheses of the Ω_{cc}^+ baryon for different data-taking periods. The uncertainties are due to the limited size of the simulated samples and the statistical uncertainties on the measured Ξ_{cc}^{++} baryon yields.

Year	α [10^{-2}]				
	$\tau = 40$ fs	$\tau = 80$ fs	$\tau = 120$ fs	$\tau = 160$ fs	$\tau = 200$ fs
2016	0.86 ± 0.17	0.46 ± 0.09	0.32 ± 0.06	0.25 ± 0.05	0.22 ± 0.04
2017	1.29 ± 0.20	0.69 ± 0.11	0.48 ± 0.07	0.38 ± 0.06	0.33 ± 0.05
2018	1.26 ± 0.18	0.67 ± 0.10	0.47 ± 0.07	0.37 ± 0.05	0.32 ± 0.05

Dalitz distributions of the simulated intermediate Ξ_c^+ (Λ_c^+) states are corrected to match those in data. The tracking and PID efficiencies for both normalisation and signal modes are corrected using calibration data samples [59–61]. The efficiency ratios of both trigger categories for different data-taking periods are summarised in Table 2. Since there is an additional track in the Ξ_{cc}^{++} decay when compared to the Ω_{cc}^+ decay, the reconstruction and selection efficiency of Ξ_{cc}^{++} candidates is significantly lower. The increase in the efficiency ratio for the 2017 and 2018 data is due to the optimisation of the Ξ_{cc}^{++} online selection, following the observation of the Ξ_{cc}^{++} baryon [8].

In order to take into account the dependence of the selection efficiency upon the unknown value of the Ω_{cc}^+ lifetime, simulated Ω_{cc}^+ events are weighted to reproduce different exponential decay time distributions corresponding to lifetimes of 40, 80, 120, 160, and 200 fs. This method is used to estimate the change in the efficiency. The single-event sensitivities are calculated by the ratio of Ξ_{cc}^{++} efficiency to the Ω_{cc}^+ efficiency with different lifetime hypotheses, as shown in Tables 3 and 4, for both trigger categories.

The Ω_{cc}^+ mass is also unknown. To test the effects of different mass hypotheses, two simulated samples are generated with $m(\Omega_{cc}^+) = 3638 \text{ MeV}/c^2$ and $m(\Omega_{cc}^+) = 3838 \text{ MeV}/c^2$. These samples are used to weight the p_T distributions of final states in the Ω_{cc}^+ decay to match those in the other mass hypotheses, and the efficiency is recalculated with the weighted samples. When varying the Ω_{cc}^+ mass, it is found that the efficiency is constant; therefore, the Ω_{cc}^+ mass dependence is neglected in the evaluation of the single-event sensitivities.

Table 4: Single-event sensitivity $\alpha(\Xi_{cc}^{++}) [10^{-2}]$ of the Ξ_{cc}^{++} normalisation mode triggered exclusively by particles unrelated to the Ω_{cc}^+ (Ξ_{cc}^{++}) decay products for different lifetime hypotheses of the Ω_{cc}^+ baryon in the different data-taking periods. The uncertainties are due to the limited size of the simulated samples and the statistical uncertainty on the measured Ξ_{cc}^{++} baryon yield.

Year	$\alpha [10^{-2}]$				
	$\tau = 40$ fs	$\tau = 80$ fs	$\tau = 120$ fs	$\tau = 160$ fs	$\tau = 200$ fs
2016	0.71 ± 0.11	0.35 ± 0.06	0.22 ± 0.04	0.17 ± 0.03	0.14 ± 0.02
2017	1.16 ± 0.12	0.57 ± 0.06	0.37 ± 0.04	0.28 ± 0.03	0.23 ± 0.02
2018	0.82 ± 0.08	0.41 ± 0.04	0.26 ± 0.02	0.20 ± 0.02	0.17 ± 0.02

6 Systematic uncertainties

The sources of systematic uncertainties on the production ratio R are listed in Table 5, where individual sources are assumed to be independent and summed in quadrature to compute the total systematic uncertainty.

The choice of the mass models used to fit the invariant mass distribution affects the normalisation yields and therefore affects the calculation of single-event sensitivities. The related systematic uncertainty is studied by using alternative functions to describe the signal and background shapes of the Ξ_{cc}^{++} mode. The sum of two Gaussian functions is chosen as an alternative signal model and a second-order polynomial function is chosen to substitute the background model. The difference in the signal yields obtained by changing models is assigned as the systematic uncertainty.

The systematic uncertainty associated with the trigger efficiency is evaluated using a tag-and-probe method [41]. The size of the normalisation sample is insufficient to derive this systematic uncertainty. Instead, b -flavoured hadrons decaying with similar final-state topologies are used. For the TOS category, $\Lambda_b^0 \rightarrow \Lambda_c^+ \pi^+ \pi^- \pi^-$ and $\Lambda_b^0 \rightarrow \Lambda_c^+ \pi^-$ candidates can be triggered by the energy deposit in the calorimeter by one of the Λ_c^+ decay products, which are similar to the $\Xi_{cc}^{++} \rightarrow \Lambda_c^+ K^- \pi^+ \pi^+$ and $\Omega_{cc}^+ \rightarrow \Xi_c^+ K^- \pi^+$ decays. The efficiency ratio of these two Λ_b^0 modes is estimated and the difference of the ratio between data and simulation is assigned as a systematic uncertainty. For the exTIS category, the $B_c^+ \rightarrow J/\psi \pi^+$ decay, which has two heavy-flavour particles (b - and c -hadrons) and is similar to the signal topology, is used to study the trigger efficiency with particle candidates that are independent and unrelated to the signal. The systematic uncertainty for the exTIS trigger category is assigned as the difference in the efficiency ratio of $\Lambda_b^0 \rightarrow \Lambda_c^+ \pi^+ \pi^- \pi^-$ mode to $B_c^+ \rightarrow J/\psi \pi^+$ mode in data and in simulation.

The tracking efficiency is corrected with calibration data samples [59], and is affected by three sources of systematic uncertainties. First, the inaccuracy of the simulation in terms of detector occupancy, which is assigned as 1.5% and 2.5% for kaons and pions, does not cancel in the ratio. An additional systematic uncertainty arises from the calibration method which provides a 0.8% uncertainty per track [59]. The third uncertainty is due to the limited size of the calibration samples and studied by pseudoexperiments. The tracking efficiency is corrected by the pseudoexperiments and the Gaussian width of the newly obtained distribution of the efficiency ratio is assigned as the systematic uncertainty.

The PID efficiency is determined in intervals of particle momentum, pseudorapidity and event multiplicity using calibration data samples. The corresponding sources of

Table 5: Systematic uncertainties on the production ratio R .

Source	R [%]
Fit model	3.5
Hardware trigger	11.2
Tracking	2.7
PID	0.9
Ξ_{cc}^{++} lifetime	12.0
Simulation/data difference	5.0
Total	17.7

systematic uncertainty are due to the limited size of the calibration samples and the binning scheme used. To study their effects, a large number of pseudoexperiments are performed, and the binning scheme is varied.

The Ξ_{cc}^{++} lifetime is measured with limited precision, 256_{-22}^{+24} (stat) ± 14 (syst) fs [62], which is propagated to the systematic uncertainty in the efficiency.

As the agreement between data and simulation is limited, a difference of 5.0% is found among different periods of data-taking, which is taken as systematic uncertainty.

7 Results

Upper limits on the production ratio R are set with a simultaneous fit to the $m(\Xi_c^+ K^- \pi^+)$ distributions of different trigger categories for all the data sets from 2016 to 2018, following the strategy described in Sec. 4 for the normalisation mode. The upper limit values are calculated by setting different Ω_{cc}^+ mass hypotheses in the fit within the $m(\Xi_c^+ K^- \pi^+)$ mass range from 3600 to 4000 MeV/ c^2 with a step of 2 MeV/ c^2 , for five different lifetime hypotheses, 40, 80, 120, 160, and 200 fs.

For each Ω_{cc}^+ mass and lifetime hypothesis, the likelihood profile is determined as a function of R . It is then convolved with a Gaussian distribution whose width is equal to the square root of the quadratic combination of the statistical and systematic uncertainties on the single-event sensitivity. The upper limit at 95% credibility level is defined as the value of R at which the integral of the profile likelihood equals 95% of the total area. Figure 6 shows the 95% credibility level upper limits at different mass hypotheses for five different lifetimes. The upper limits on R decrease when increasing the Ω_{cc}^+ lifetime. Considering the whole explored mass range, the highest upper limit on R is 0.11 obtained under lifetime hypothesis of 40 fs while the lowest is 0.5×10^{-2} obtained under lifetime hypothesis of 200 fs.

8 Conclusion

A search for the Ω_{cc}^+ baryon through the $\Xi_c^+ K^- \pi^+$ decay is performed, using pp collision data collected by the LHCb experiment from 2016 to 2018 at a centre-of-mass energy of 13 TeV, corresponding to an integrated luminosity of 5.4 fb^{-1} . No significant signal is observed in the mass range of 3.6 to 4.0 GeV/ c^2 . Upper limits are set at 95% credibility

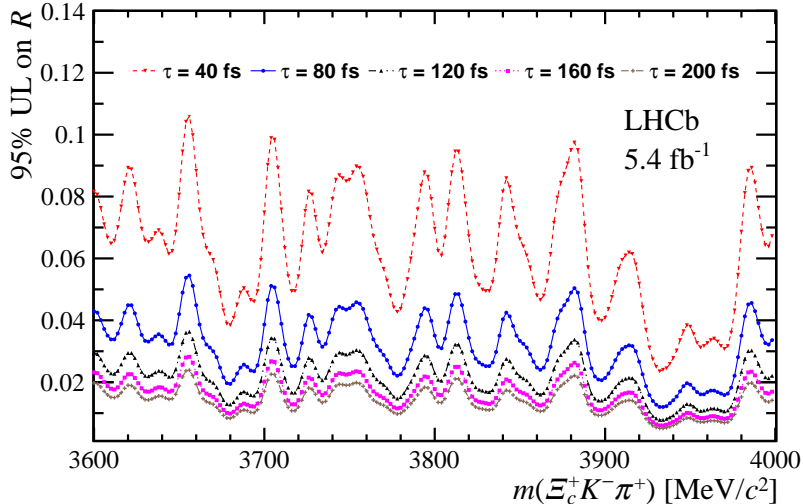


Figure 6: Upper limits on the production ratio R at 95% credibility level as a function of $m(\Xi_c^+ K^- \pi^+)$ at $\sqrt{s} = 13$ TeV, for five Ω_{cc}^+ lifetime hypotheses.

level on the ratio of the Ω_{cc}^+ production cross-section times the branching fraction to that of the Ξ_{cc}^{++} baryon as a function of the Ω_{cc}^+ mass and for different lifetime hypotheses, in the rapidity range of 2.0 to 4.5 and the transverse momentum range of 4 to 15 GeV/ c . The upper limits are set assuming that the $\Omega_{cc}^+ \rightarrow \Xi_c^+ K^- \pi^+$ decay proceeds according to a uniform phase-space model. The upper limits depend strongly on the mass and lifetime hypotheses of the Ω_{cc}^+ , and vary from 1.1×10^{-1} to 0.5×10^{-2} for 40 fs to 200 fs, respectively. Future searches by the LHCb experiment with upgraded detectors, improved trigger conditions, additional Ω_{cc}^+ decay modes, and larger data samples will further increase the Ω_{cc}^+ signal sensitivity.

Acknowledgements

We express our gratitude to our colleagues in the CERN accelerator departments for the excellent performance of the LHC. We thank the technical and administrative staff at the LHCb institutes. We acknowledge support from CERN and from the national agencies: CAPES, CNPq, FAPERJ and FINEP (Brazil); MOST and NSFC (China); CNRS/IN2P3 (France); BMBF, DFG and MPG (Germany); INFN (Italy); NWO (Netherlands); MNiSW and NCN (Poland); MEN/IFA (Romania); MSHE (Russia); MICINN (Spain); SNSF and SER (Switzerland); NASU (Ukraine); STFC (United Kingdom); DOE NP and NSF (USA). We acknowledge the computing resources that are provided by CERN, IN2P3 (France), KIT and DESY (Germany), INFN (Italy), SURF (Netherlands), PIC (Spain), GridPP (United Kingdom), RRCKI and Yandex LLC (Russia), CSCS (Switzerland), IFIN-HH (Romania), CBPF (Brazil), PL-GRID (Poland) and NERSC (USA). We are indebted to the communities behind the multiple open-source software packages on which we depend. Individual groups or members have received support from ARC and ARDC (Australia); AvH Foundation (Germany); EPLANET, Marie Skłodowska-Curie Actions and ERC (European Union); A*MIDEX, ANR, IPhU and Labex P2IO, and Région Auvergne-Rhône-Alpes (France); Key Research Program of Frontier Sciences of CAS, CAS

PIFI, CAS CCEPP, Fundamental Research Funds for the Central Universities, and Sci. & Tech. Program of Guangzhou (China); RFBR, RSF and Yandex LLC (Russia); GVA, XuntaGal and GENCAT (Spain); the Leverhulme Trust, the Royal Society and UKRI (United Kingdom).

References

- [1] M. Gell-Mann, *A Schematic Model of Baryons and Mesons*, Phys. Lett. **8** (1964) 214.
- [2] G. Zweig, *An $SU(3)$ model for strong interaction symmetry and its breaking, Part 1*, CERN-TH-401 (1964).
- [3] G. Zweig, *An $SU(3)$ model for strong interaction symmetry and its breaking, Part 2*, CERN-TH-412 (1964).
- [4] S. Fleck and J.-M. Richard, *Baryons with double charm*, Prog. Theor. Phys. **82** (1989) 760.
- [5] A. V. Berezhnoy, V. V. Kiselev, A. K. Likhoded, and A. I. Onishchenko, *Doubly charmed baryon production in hadronic experiments*, Phys. Rev. **D57** (1998) 4385, [arXiv:hep-ph/9710339](#).
- [6] D. Ebert, R. N. Faustov, V. O. Galkin, and A. P. Martynenko, *Mass spectra of doubly heavy baryons in the relativistic quark model*, Phys. Rev. **D66** (2002) 014008, [arXiv:hep-ph/0201217](#).
- [7] C.-H. Chang, C.-F. Qiao, J.-X. Wang, and X.-G. Wu, *Estimate of the hadronic production of the doubly charmed baryon Ξ_{cc} under GM-VFN scheme*, Phys. Rev. **D73** (2006) 094022, [arXiv:hep-ph/0601032](#).
- [8] LHCb collaboration, R. Aaij *et al.*, *Observation of the doubly charmed baryon Ξ_{cc}^{++}* , Phys. Rev. Lett. **119** (2017) 112001, [arXiv:1707.01621](#).
- [9] LHCb collaboration, R. Aaij *et al.*, *First observation of the doubly charmed baryon decay $\Xi_{cc}^{++} \rightarrow \Xi_c^+ \pi^+$* , Phys. Rev. Lett. **121** (2018) 162002, [arXiv:1807.01919](#).
- [10] LHCb collaboration, R. Aaij *et al.*, *Search for the doubly charmed baryon Ξ_{cc}^+* , Sci. China Phys. Mech. Astron. **63** (2020) 221062, [arXiv:1909.12273](#).
- [11] S. S. Gershtein, V. V. Kiselev, A. K. Likhoded, and A. I. Onishchenko, *Spectroscopy of doubly heavy baryons*, Phys. Rev. **D62** (2000) 054021, [arXiv:hep-ph/9811212](#).
- [12] D. Ebert *et al.*, *Heavy baryons in the relativistic quark model*, Phys. **C76** (1997) 111, [arXiv:hep-ph/9607314](#).
- [13] R. Roncaglia, A. Dzierba, D. B. Lichtenberg, and E. Predazzi, *Predicting the masses of heavy hadrons without an explicit Hamiltonian*, Phys. Rev. **D51** (1995) 1248, [arXiv:hep-ph/9405392](#).
- [14] R. Roncaglia, D. B. Lichtenberg, and E. Predazzi, *Predicting the masses of baryons containing one or two heavy quarks*, Phys. Rev. **D52** (1995) 1722, [arXiv:hep-ph/9502251](#).
- [15] J. G. Koerner, D. Pirjol, and M. Kraemer, *Heavy baryons*, Prog. Part. Nucl. Phys. **33** (1994) 787, [arXiv:hep-ph/9406359](#).

- [16] I. M. Narodetskii and M. A. Trusov, *The heavy baryons in the nonperturbative string approach*, Phys. Atom. Nucl. **65** (2002) 917, arXiv:hep-ph/0104019.
- [17] S. B. Zachary, W. Detmold, S. Meinel, and K. Orginos, *Charmed bottom baryon spectroscopy from lattice QCD*, Phys. Rev. **D90** (2014) 094507, arXiv:1409.0497.
- [18] T. M. Aliev, K. Azizi, and M. Savci, *Doubly Heavy Spin-1/2 Baryon Spectrum in QCD*, Nucl. Phys. **A895** (2012) 59, arXiv:1205.2873.
- [19] A. Valcarce, H. Garcilazo, and J. Vijande, *Towards an understanding of heavy baryon spectroscopy*, Eur. Phys. **A37** (2008) 217, arXiv:0807.2973.
- [20] J. Vijande, A. Valcarce, T. F. Caramés, and H. Garcilazo, *Heavy hadron spectroscopy: A quark model perspective*, Int. J. Mod. Phys. **E22** (2013) 1130011, arXiv:1212.4383.
- [21] H.-Y. Cheng and Y.-L. Shi, *Lifetimes of doubly charmed baryons*, Phys. Rev. **D98** (2018) 113005, arXiv:1809.08102.
- [22] C.-H. Chang, T. Li, X.-Q. Li, and Y.-M. Wang, *Lifetime of doubly charmed baryons*, Commun. Theor. Phys. **49** (2008) 993, arXiv:0704.0016.
- [23] B. Guberina, B. Melic, and H. Stefancic, *Inclusive decays and lifetimes of doubly charmed baryons*, Eur. Phys. J. **C9** (1999) 213, arXiv:hep-ph/9901323.
- [24] M. Karliner and J. L. Rosner, *Baryons with two heavy quarks: Masses, production, decays, and detection*, Phys. Rev. **D90** (2014) 094007, arXiv:1408.5877.
- [25] V. V. Kiselev, A. K. Likhoded, and A. I. Onishchenko, *Lifetimes of doubly charmed baryons: Ξ_{cc}^+ and Ξ_{cc}^{++}* , Phys. Rev. **D60** (1999) 014007, arXiv:hep-ph/9807354.
- [26] V. V. Kiselev and A. K. Likhoded, *Baryons with two heavy quarks*, Phys. Usp. **45** (2002) 455, arXiv:hep-ph/0103169, [Usp. Fiz. Nauk 172,497(2002)].
- [27] J. P. Ma and Z. G. Si, *Factorization approach for inclusive production of doubly heavy baryon*, Phys. Lett. **B568** (2003) 135, arXiv:hep-ph/0305079.
- [28] C.-H. Chang, J.-P. Ma, C.-F. Qiao, and X.-G. Wu, *Hadronic production of the doubly charmed baryon Ξ_{cc} with intrinsic charm*, J. Phys. **G34** (2007) 845, arXiv:hep-ph/0610205.
- [29] J.-W. Zhang *et al.*, *Hadronic production of the doubly heavy baryon Ξ_{bc} at LHC*, Phys. Rev. **D83** (2011) 034026, arXiv:1101.1130.
- [30] C.-H. Chang, C.-F. Qiao, J.-X. Wang, and X.-G. Wu, *The color-octet contributions to P-wave B_c meson hadroproduction*, Phys. Rev. **D71** (2005) 074012, arXiv:hep-ph/0502155.
- [31] LHCb collaboration, R. Aaij *et al.*, *Measurement of Ξ_{cc}^{++} production in pp collisions at $\sqrt{s} = 13$ TeV*, Chin. Phys. **C44** (2020) 022001, arXiv:1910.11316.
- [32] A. V. Berezhnoy, A. K. LikhoAded, and A. V. Luchinsky, *Doubly heavy baryons at the LHC*, Phys. Rev. **D98** (2018) 113004, arXiv:1809.10058.

- [33] Y.-J. Shi, W. Wang, Y. Xing, and J. Xu, *Weak decays of doubly heavy baryons: Multi-body decay channels*, Eur. Phys. J. **C78** (2018) 56, arXiv:1712.03830.
- [34] L.-J. Jiang, B. He, and R.-H. Li, *Weak decays of doubly heavy baryons: $\mathcal{B}_{cc} \rightarrow \mathcal{B}_c V$* , Eur. Phys. J. **C78** (2018) 961, arXiv:1810.00541.
- [35] LHCb collaboration, A. A. Alves Jr. *et al.*, *The LHCb detector at the LHC*, JINST **3** (2008) S08005.
- [36] LHCb collaboration, R. Aaij *et al.*, *LHCb detector performance*, Int. J. Mod. Phys. **A30** (2015) 1530022, arXiv:1412.6352.
- [37] R. Aaij *et al.*, *Performance of the LHCb Vertex Locator*, JINST **9** (2014) P09007, arXiv:1405.7808.
- [38] R. Arink *et al.*, *Performance of the LHCb Outer Tracker*, JINST **9** (2014) P01002, arXiv:1311.3893.
- [39] P. d'Argent *et al.*, *Improved performance of the LHCb Outer Tracker in LHC Run 2*, JINST **12** (2017) P11016, arXiv:1708.00819.
- [40] M. Adinolfi *et al.*, *Performance of the LHCb RICH detector at the LHC*, Eur. Phys. J. **C73** (2013) 2431, arXiv:1211.6759.
- [41] R. Aaij *et al.*, *The LHCb trigger and its performance in 2011*, JINST **8** (2013) P04022, arXiv:1211.3055.
- [42] T. Sjöstrand, S. Mrenna, and P. Skands, *A brief introduction to PYTHIA 8.1*, Comput. Phys. Commun. **178** (2008) 852, arXiv:0710.3820; T. Sjöstrand, S. Mrenna, and P. Skands, *PYTHIA 6.4 physics and manual*, JHEP **05** (2006) 026, arXiv:hep-ph/0603175.
- [43] I. Belyaev *et al.*, *Handling of the generation of primary events in Gauss, the LHCb simulation framework*, J. Phys. Conf. Ser. **331** (2011) 032047.
- [44] C.-H. Chang, J.-X. Wang, and X.-G. Wu, *GENXICC2.0: an upgraded version of the generator for hadronic production of double heavy baryons Ξ_{cc} , Ξ_{bc} and Ξ_{bb}* , Comput. Phys. Commun. **181** (2010) 1144, arXiv:0910.4462.
- [45] D. J. Lange, *The EvtGen particle decay simulation package*, Nucl. Instrum. Meth. **A462** (2001) 152.
- [46] N. Davidson, T. Przedzinski, and Z. Was, *PHOTOS interface in C++: Technical and physics documentation*, Comp. Phys. Comm. **199** (2016) 86, arXiv:1011.0937.
- [47] Geant4 collaboration, J. Allison *et al.*, *Geant4 developments and applications*, IEEE Trans. Nucl. Sci. **53** (2006) 270; Geant4 collaboration, S. Agostinelli *et al.*, *Geant4: A simulation toolkit*, Nucl. Instrum. Meth. **A506** (2003) 250.
- [48] M. Clemencic *et al.*, *The LHCb simulation application, Gauss: Design, evolution and experience*, J. Phys. Conf. Ser. **331** (2011) 032023.

- [49] A. Gulin, I. Kuralenok, and D. Pavlov, *Winning The Transfer Learning Track of Yahoo!'s Learning To Rank Challenge with YetiRank*, in *Proceedings of the Learning to Rank Challenge*, **14**, 63–76, PMLR, 2011.
- [50] T. Likhomanenko *et al.*, *LHCb topological trigger reoptimization*, J. Phys. Conf. Ser. **664** (2015) 082025.
- [51] Particle Data Group, P. A. Zyla *et al.*, *Review of particle physics*, Prog. Theor. Exp. Phys. **2020** (2020) 083C01.
- [52] L. Breiman, J. H. Friedman, R. A. Olshen, and C. J. Stone, *Classification and regression trees*, Wadsworth international group, Belmont, California, USA, 1984.
- [53] H. Voss, A. Hoecker, J. Stelzer, and F. Tegenfeldt, *TMVA - Toolkit for Multivariate Data Analysis with ROOT*, PoS **ACAT** (2007) 040; A. Hoecker *et al.*, *TMVA 4 — Toolkit for Multivariate Data Analysis with ROOT. Users Guide.*, arXiv:physics/0703039.
- [54] G. Punzi, *Sensitivity of searches for new signals and its optimization*, eConf **C030908** (2003) MODT002, arXiv:physics/0308063.
- [55] T. Skwarnicki, *A study of the radiative cascade transitions between the Upsilon-prime and Upsilon resonances*, PhD thesis, Institute of Nuclear Physics, Krakow, 1986, DESY-F31-86-02.
- [56] S. S. Wilks, *The large-sample distribution of the likelihood ratio for testing composite hypotheses*, Ann. Math. Stat. **9** (1938) 60.
- [57] I. Narsky, *Estimation of upper limits using a Poisson statistic*, Nucl. Instrum. Meth. **A450** (2000) 444, arXiv:9904025.
- [58] E. Gross and O. Vitells, *Trial factors for the look elsewhere effect in high energy physics*, Eur. Phys. J. **C70** (2010) 525, arXiv:1005.1891.
- [59] LHCb collaboration, R. Aaij *et al.*, *Measurement of the track reconstruction efficiency at LHCb*, JINST **10** (2015) P02007, arXiv:1408.1251.
- [60] L. Anderlini *et al.*, *The PIDCalib package*, LHCb-PUB-2016-021, 2016.
- [61] R. Aaij *et al.*, *Selection and processing of calibration samples to measure the particle identification performance of the LHCb experiment in Run 2*, Eur. Phys. J. Tech. Instr. **6** (2018) 1, arXiv:1803.00824.
- [62] LHCb collaboration, R. Aaij *et al.*, *Measurement of the lifetime of the doubly charmed baryon Ξ_{cc}^{++}* , Phys. Rev. Lett. **121** (2018) 052002, arXiv:1806.02744.

LHCb collaboration

R. Aaij³², C. Abellán Beteta⁵⁰, T. Ackernley⁶⁰, B. Adeva⁴⁶, M. Adinolfi⁵⁴, H. Afsharnia⁹, C.A. Aidala⁸⁶, S. Aiola²⁵, Z. Ajaltouni⁹, S. Akar⁶⁵, J. Albrecht¹⁵, F. Alessio⁴⁸, M. Alexander⁵⁹, A. Alfonso Alberio⁴⁵, Z. Aliouche⁶², G. Alkhazov³⁸, P. Alvarez Cartelle⁵⁵, S. Amato², Y. Amhis¹¹, L. An⁴⁸, L. Anderlini²², A. Andreianov³⁸, M. Andreotti²¹, F. Archilli¹⁷, A. Artamonov⁴⁴, M. Artuso⁶⁸, K. Arzymatov⁴², E. Aslanides¹⁰, M. Atzeni⁵⁰, B. Audurier¹², S. Bachmann¹⁷, M. Bachmayer⁴⁹, J.J. Back⁵⁶, P. Baladron Rodriguez⁴⁶, V. Balagura¹², W. Baldini²¹, J. Baptista Leite¹, R.J. Barlow⁶², S. Barsuk¹¹, W. Barter⁶¹, M. Bartolini²⁴, F. Baryshnikov⁸³, J.M. Basels¹⁴, G. Bassi²⁹, B. Batsukh⁶⁸, A. Battig¹⁵, A. Bay⁴⁹, M. Becker¹⁵, F. Bedeschi²⁹, I. Bediaga¹, A. Beiter⁶⁸, V. Belavin⁴², S. Belin²⁷, V. Bellee⁴⁹, K. Belous⁴⁴, I. Belov⁴⁰, I. Belyaev⁴¹, G. Bencivenni²³, E. Ben-Haim¹³, A. Berezhnoy⁴⁰, R. Bernet⁵⁰, D. Berninghoff¹⁷, H.C. Bernstein⁶⁸, C. Bertella⁴⁸, A. Bertolin²⁸, C. Betancourt⁵⁰, F. Betti⁴⁸, Ia. Bezshyiko⁵⁰, S. Bhasin⁵⁴, J. Bhom³⁵, L. Bian⁷³, M.S. Bieker¹⁵, S. Bifani⁵³, P. Billoir¹³, M. Birch⁶¹, F.C.R. Bishop⁵⁵, A. Bitadze⁶², A. Bizzeti^{22,k}, M. Bjørn⁶³, M.P. Blago⁴⁸, T. Blake⁵⁶, F. Blanc⁴⁹, S. Blusk⁶⁸, D. Bobulska⁵⁹, J.A. Boelhauve¹⁵, O. Boente Garcia⁴⁶, T. Boettcher⁶⁵, A. Boldyrev⁸², A. Bondar⁴³, N. Bondar^{38,48}, S. Borghi⁶², M. Borisyak⁴², M. Borsato¹⁷, J.T. Borsuk³⁵, S.A. Bouchiba⁴⁹, T.J.V. Bowcock⁶⁰, A. Boyer⁴⁸, C. Bozzi²¹, M.J. Bradley⁶¹, S. Braun⁶⁶, A. Brea Rodriguez⁴⁶, M. Brodski⁴⁸, J. Brodzicka³⁵, A. Brossa Gonzalo⁵⁶, D. Brundu²⁷, A. Buonaura⁵⁰, C. Burr⁴⁸, A. Bursche⁷², A. Butkevich³⁹, J.S. Butter³², J. Buytaert⁴⁸, W. Byczynski⁴⁸, S. Cadeddu²⁷, H. Cai⁷³, R. Calabrese^{21,f}, L. Calefice^{15,13}, L. Calero Diaz²³, S. Cali²³, R. Calladine⁵³, M. Calvi^{26,j}, M. Calvo Gomez⁸⁵, P. Camargo Magalhaes⁵⁴, P. Campana²³, A.F. Campoverde Quezada⁶, S. Capelli^{26,j}, L. Capriotti^{20,d}, A. Carbone^{20,d}, G. Carboni³¹, R. Cardinale²⁴, A. Cardini²⁷, I. Carli⁴, P. Carniti^{26,j}, L. Carus¹⁴, K. Carvalho Akiba³², A. Casais Vidal⁴⁶, G. Casse⁶⁰, M. Cattaneo⁴⁸, G. Cavallero⁴⁸, S. Celani⁴⁹, J. Cerasoli¹⁰, A.J. Chadwick⁶⁰, M.G. Chapman⁵⁴, M. Charles¹³, Ph. Charpentier⁴⁸, G. Chatzikonstantinidis⁵³, C.A. Chavez Barajas⁶⁰, M. Chefdeville⁸, C. Chen³, S. Chen⁴, A. Chernov³⁵, V. Chobanova⁴⁶, S. Cholak⁴⁹, M. Chruszcz³⁵, A. Chubykin³⁸, V. Chulikov³⁸, P. Ciambrone²³, M.F. Cicala⁵⁶, X. Cid Vidal⁴⁶, G. Ciezarek⁴⁸, P.E.L. Clarke⁵⁸, M. Clemencic⁴⁸, H.V. Cliff⁵⁵, J. Closier⁴⁸, J.L. Cobbedick⁶², V. Coco⁴⁸, J.A.B. Coelho¹¹, J. Cogan¹⁰, E. Cogneras⁹, L. Cojocariu³⁷, P. Collins⁴⁸, T. Colombo⁴⁸, L. Congedo^{19,c}, A. Contu²⁷, N. Cooke⁵³, G. Coombs⁵⁹, G. Corti⁴⁸, C.M. Costa Sobral⁵⁶, B. Couturier⁴⁸, D.C. Craik⁶⁴, J. Crkovská⁶⁷, M. Cruz Torres¹, R. Currie⁵⁸, C.L. Da Silva⁶⁷, S. Dadabaev⁸³, E. Dall'Occo¹⁵, J. Dalseno⁴⁶, C. D'Ambrosio⁴⁸, A. Danilina⁴¹, P. d'Argent⁴⁸, A. Davis⁶², O. De Aguiar Francisco⁶², K. De Bruyn⁷⁹, S. De Capua⁶², M. De Cian⁴⁹, J.M. De Miranda¹, L. De Paula², M. De Serio^{19,c}, D. De Simone⁵⁰, P. De Simone²³, J.A. de Vries⁸⁰, C.T. Dean⁶⁷, D. Decamp⁸, L. Del Buono¹³, B. Delaney⁵⁵, H.-P. Dembinski¹⁵, A. Dendek³⁴, V. Denysenko⁵⁰, D. Derkach⁸², O. Deschamps⁹, F. Desse¹¹, F. Dettori^{27,e}, B. Dey⁷⁷, A. Di Cicco²³, P. Di Nezza²³, S. Didenko⁸³, L. Dieste Maronas⁴⁶, H. Dijkstra⁴⁸, V. Dobishuk⁵², A.M. Donohoe¹⁸, F. Dordei²⁷, A.C. dos Reis¹, L. Douglas⁵⁹, A. Dovbnya⁵¹, A.G. Downes⁸, K. Dreimanis⁶⁰, M.W. Dudek³⁵, L. Dufour⁴⁸, V. Duk⁷⁸, P. Durante⁴⁸, J.M. Durham⁶⁷, D. Dutta⁶², A. Dziurda³⁵, A. Dzyuba³⁸, S. Easo⁵⁷, U. Egede⁶⁹, V. Egorychev⁴¹, S. Eidelman^{43,v}, S. Eisenhardt⁵⁸, S. Ek-In⁴⁹, L. Eklund^{59,w}, S. Ely⁶⁸, A. Ene³⁷, E. Epple⁶⁷, S. Escher¹⁴, J. Eschle⁵⁰, S. Esen¹³, T. Evans⁴⁸, A. Falabella²⁰, J. Fan³, Y. Fan⁶, B. Fang⁷³, S. Farry⁶⁰, D. Fazzini^{26,j}, M. Féo⁴⁸, A. Fernandez Prieto⁴⁶, J.M. Fernandez-tenllado Arribas⁴⁵, A.D. Fernez⁶⁶, F. Ferrari^{20,d}, L. Ferreira Lopes⁴⁹, F. Ferreira Rodrigues², S. Ferreres Sole³², M. Ferrillo⁵⁰, M. Ferro-Luzzi⁴⁸, S. Filippov³⁹, R.A. Fini¹⁹, M. Fiorini^{21,f}, M. Firlej³⁴, K.M. Fischer⁶³, D.S. Fitzgerald⁸⁶, C. Fitzpatrick⁶², T. Fiutowski³⁴, A. Fkiaras⁴⁸, F. Fleuret¹², M. Fontana¹³, F. Fontanelli^{24,h}, R. Forty⁴⁸, V. Franco Lima⁶⁰, M. Franco Sevilla⁶⁶, M. Frank⁴⁸, E. Franzoso²¹, G. Frau¹⁷, C. Frei⁴⁸, D.A. Friday⁵⁹, J. Fu²⁵, Q. Fuehring¹⁵, W. Funk⁴⁸,

E. Gabriel³², T. Gaintseva⁴², A. Gallas Torreira⁴⁶, D. Galli^{20,d}, S. Gambetta^{58,48}, Y. Gan³,
 M. Gandelman², P. Gandini²⁵, Y. Gao⁵, M. Garau²⁷, L.M. Garcia Martin⁵⁶,
 P. Garcia Moreno⁴⁵, J. García Pardiñas^{26,j}, B. Garcia Plana⁴⁶, F.A. Garcia Rosales¹²,
 L. Garrido⁴⁵, C. Gaspar⁴⁸, R.E. Geertsema³², D. Gerick¹⁷, L.L. Gerken¹⁵, E. Gersabeck⁶²,
 M. Gersabeck⁶², T. Gershon⁵⁶, D. Gerstel¹⁰, Ph. Ghez⁸, V. Gibson⁵⁵, H.K. Giemza³⁶,
 M. Giovannetti^{23,p}, A. Gioventù⁴⁶, P. Gironella Gironell⁴⁵, L. Giubega³⁷, C. Giugliano^{21,f,48},
 K. Gizdov⁵⁸, E.L. Gkougkousis⁴⁸, V.V. Gligorov¹³, C. Göbel⁷⁰, E. Golobardes⁸⁵, D. Golubkov⁴¹,
 A. Golutvin^{61,83}, A. Gomes^{1,a}, S. Gomez Fernandez⁴⁵, F. Goncalves Abrantes⁶³, M. Goncerz³⁵,
 G. Gong³, P. Gorbounov⁴¹, I.V. Gorelov⁴⁰, C. Gotti²⁶, E. Govorkova⁴⁸, J.P. Grabowski¹⁷,
 T. Grammatico¹³, L.A. Granado Cardoso⁴⁸, E. Graugés⁴⁵, E. Graverini⁴⁹, G. Graziani²²,
 A. Grecu³⁷, L.M. Greeven³², P. Griffith^{21,f}, L. Grillo⁶², S. Gromov⁸³, B.R. Gruberg Cazon⁶³,
 C. Gu³, M. Guarise²¹, P. A. Günther¹⁷, E. Gushchin³⁹, A. Guth¹⁴, Y. Guz⁴⁴, T. Gys⁴⁸,
 T. Hadavizadeh⁶⁹, G. Haefeli⁴⁹, C. Haen⁴⁸, J. Haimberger⁴⁸, T. Halewood-leagas⁶⁰,
 P.M. Hamilton⁶⁶, J.P. Hammerich⁶⁰, Q. Han⁷, X. Han¹⁷, T.H. Hancock⁶³,
 S. Hansmann-Menzemer¹⁷, N. Harnew⁶³, T. Harrison⁶⁰, C. Hasse⁴⁸, M. Hatch⁴⁸, J. He^{6,b},
 M. Hecker⁶¹, K. Heijhoff³², K. Heinicke¹⁵, A.M. Hennequin⁴⁸, K. Hennessy⁶⁰, L. Henry⁴⁸,
 J. Heuel¹⁴, A. Hicheur², D. Hill⁴⁹, M. Hilton⁶², S.E. Hollitt¹⁵, J. Hu¹⁷, J. Hu⁷², W. Hu⁷,
 X. Hu³, W. Huang⁶, X. Huang⁷³, W. Hulsbergen³², R.J. Hunter⁵⁶, M. Hushchyn⁸²,
 D. Hutchcroft⁶⁰, D. Hynds³², P. Ibis¹⁵, M. Idzik³⁴, D. Ilin³⁸, P. Ilten⁶⁵, A. Inglessi³⁸,
 A. Ishteev⁸³, K. Ivshin³⁸, R. Jacobsson⁴⁸, S. Jakobsen⁴⁸, E. Jans³², B.K. Jashal⁴⁷,
 A. Jawahery⁶⁶, V. Jevtic¹⁵, M. Jezabek³⁵, F. Jiang³, M. John⁶³, D. Johnson⁴⁸, C.R. Jones⁵⁵,
 T.P. Jones⁵⁶, B. Jost⁴⁸, N. Jurik⁴⁸, S. Kandybei⁵¹, Y. Kang³, M. Karacson⁴⁸, M. Karpov⁸²,
 F. Keizer⁴⁸, M. Kenzie⁵⁶, T. Ketel³³, B. Khanji¹⁵, A. Kharisova⁸⁴, S. Kholodenko⁴⁴, T. Kirn¹⁴,
 V.S. Kirsebom⁴⁹, O. Kitouni⁶⁴, S. Klaver³², K. Klimaszewski³⁶, S. Koliiev⁵², A. Kondybayeva⁸³,
 A. Konoplyannikov⁴¹, P. Kopciwicz³⁴, R. Kopecna¹⁷, P. Koppenburg³², M. Korolev⁴⁰,
 I. Kostiuik^{32,52}, O. Kot⁵², S. Kotriakhova^{21,38}, P. Kravchenko³⁸, L. Kravchuk³⁹,
 R.D. Krawczyk⁴⁸, M. Kreps⁵⁶, F. Kress⁶¹, S. Kretzschmar¹⁴, P. Krokovny^{43,v}, W. Krupa³⁴,
 W. Krzemien³⁶, W. Kucewicz^{35,t}, M. Kucharczyk³⁵, V. Kudryavtsev^{43,v}, H.S. Kuindersma^{32,33},
 G.J. Kunde⁶⁷, T. Kvaratskheliya⁴¹, D. Lacarrere⁴⁸, G. Lafferty⁶², A. Lai²⁷, A. Lampis²⁷,
 D. Lancierini⁵⁰, J.J. Lane⁶², R. Lane⁵⁴, G. Lanfranchi²³, C. Langenbruch¹⁴, J. Langer¹⁵,
 O. Lantwin⁵⁰, T. Latham⁵⁶, F. Lazzari^{29,q}, R. Le Gac¹⁰, S.H. Lee⁸⁶, R. Lefèvre⁹, A. Leflat⁴⁰,
 S. Legotin⁸³, O. Leroy¹⁰, T. Lesiak³⁵, B. Leverington¹⁷, H. Li⁷², L. Li⁶³, P. Li¹⁷, S. Li⁷, Y. Li⁴,
 Y. Li⁴, Z. Li⁶⁸, X. Liang⁶⁸, T. Lin⁶¹, R. Lindner⁴⁸, V. Lisovskyi¹⁵, R. Litvinov²⁷, G. Liu⁷²,
 H. Liu⁶, S. Liu⁴, A. Loi²⁷, J. Lomba Castro⁴⁶, I. Longstaff⁵⁹, J.H. Lopes², G.H. Lovell⁵⁵, Y. Lu⁴,
 D. Lucchesi^{28,l}, S. Luchuk³⁹, M. Lucio Martinez³², V. Lukashenko³², Y. Luo³, A. Lupato⁶²,
 E. Luppi^{21,f}, O. Lupton⁵⁶, A. Lusiani^{29,m}, X. Lyu⁶, L. Ma⁴, R. Ma⁶, S. Maccolini^{20,d},
 F. Machefert¹¹, F. Maciuc³⁷, V. Macko⁴⁹, P. Mackowiak¹⁵, S. Maddrell-Mander⁵⁴,
 O. Madejczyk³⁴, L.R. Madhan Mohan⁵⁴, O. Maev³⁸, A. Maevskiy⁸², D. Maisuzenko³⁸,
 M.W. Majewski³⁴, J.J. Malczewski³⁵, S. Malde⁶³, B. Malecki⁴⁸, A. Malinin⁸¹, T. Maltsev^{43,v},
 H. Malygina¹⁷, G. Manca^{27,e}, G. Mancinelli¹⁰, D. Manuzzi^{20,d}, D. Marangotto^{25,i}, J. Maratas^{9,s},
 J.F. Marchand⁸, U. Marconi²⁰, S. Mariani^{22,g}, C. Marin Benito⁴⁸, M. Marinangeli⁴⁹, J. Marks¹⁷,
 A.M. Marshall⁵⁴, P.J. Marshall⁶⁰, G. Martellotti³⁰, L. Martinazzoli^{48,j}, M. Martinelli^{26,j},
 D. Martinez Santos⁴⁶, F. Martinez Vidal⁴⁷, A. Massafferri¹, M. Materok¹⁴, R. Matev⁴⁸,
 A. Mathad⁵⁰, Z. Mathe⁴⁸, V. Matiunin⁴¹, C. Matteuzzi²⁶, K.R. Mattioli⁸⁶, A. Mauri³²,
 E. Maurice¹², J. Mauricio⁴⁵, M. Mazurek⁴⁸, M. McCann⁶¹, L. McConnell¹⁸, T.H. Mcgrath⁶²,
 A. McNab⁶², R. McNulty¹⁸, J.V. Mead⁶⁰, B. Meadows⁶⁵, G. Meier¹⁵, N. Meinert⁷⁶,
 D. Melnychuk³⁶, S. Meloni^{26,j}, M. Merk^{32,80}, A. Merli²⁵, L. Meyer Garcia², M. Mikhasenko⁴⁸,
 D.A. Milanese⁷⁴, E. Millard⁵⁶, M. Milovanovic⁴⁸, M.-N. Minard⁸, A. Minotti²¹, L. Minzoni^{21,f},
 S.E. Mitchell⁵⁸, B. Mitreska⁶², D.S. Mitzel⁴⁸, A. Mödden¹⁵, R.A. Mohammed⁶³, R.D. Moise⁶¹,
 T. Mombächer⁴⁶, I.A. Monroy⁷⁴, S. Monteil⁹, M. Morandin²⁸, G. Morello²³, M.J. Morello^{29,m},

J. Moron³⁴, A.B. Morris⁷⁵, A.G. Morris⁵⁶, R. Mountain⁶⁸, H. Mu³, F. Muheim^{58,48},
 M. Mulder⁴⁸, D. Müller⁴⁸, K. Müller⁵⁰, C.H. Murphy⁶³, D. Murray⁶², P. Muzzetto^{27,48},
 P. Naik⁵⁴, T. Nakada⁴⁹, R. Nandakumar⁵⁷, T. Nanut⁴⁹, I. Nasteva², M. Needham⁵⁸, I. Neri²¹,
 N. Neri^{25,i}, S. Neubert⁷⁵, N. Neufeld⁴⁸, R. Newcombe⁶¹, T.D. Nguyen⁴⁹, C. Nguyen-Mau^{49,x},
 E.M. Niel¹¹, S. Nieswand¹⁴, N. Nikitin⁴⁰, N.S. Nolte⁶⁴, C. Normand⁸, C. Nunez⁸⁶,
 A. Oblakowska-Mucha³⁴, V. Obraztsov⁴⁴, D.P. O’Hanlon⁵⁴, R. Oldeman^{27,e}, M.E. Olivares⁶⁸,
 C.J.G. Onderwater⁷⁹, R.H. O’neil⁵⁸, A. Ossowska³⁵, J.M. Otalora Goicochea²,
 T. Ovsianikova⁴¹, P. Owen⁵⁰, A. Oyanguren⁴⁷, B. Pagare⁵⁶, P.R. Pais⁴⁸, T. Pajero⁶³,
 A. Palano¹⁹, M. Palutan²³, Y. Pan⁶², G. Panshin⁸⁴, A. Papanestis⁵⁷, M. Pappagallo^{19,c},
 L.L. Pappalardo^{21,f}, C. Pappenheimer⁶⁵, W. Parker⁶⁶, C. Parkes⁶², C.J. Parkinson⁴⁶,
 B. Passalacqua²¹, G. Passaleva²², A. Pastore¹⁹, M. Patel⁶¹, C. Patrignani^{20,d}, C.J. Pawley⁸⁰,
 A. Pearce⁴⁸, A. Pellegrino³², M. Pepe Altarelli⁴⁸, S. Perazzini²⁰, D. Pereima⁴¹, P. Perret⁹,
 M. Petric^{59,48}, K. Petridis⁵⁴, A. Petrolini^{24,h}, A. Petrov⁸¹, S. Petrucci⁵⁸, M. Petruzzo²⁵,
 T.T.H. Pham⁶⁸, A. Philippov⁴², L. Pica^{29,m}, M. Piccini⁷⁸, B. Pietrzyk⁸, G. Pietrzyk⁴⁹,
 M. Pili⁶³, D. Pinci³⁰, F. Pisani⁴⁸, Resmi P.K¹⁰, V. Placinta³⁷, J. Plews⁵³, M. Plo Casasus⁴⁶,
 F. Polci¹³, M. Poli Lener²³, M. Poliakova⁶⁸, A. Poluektov¹⁰, N. Polukhina^{83,u}, I. Polyakov⁶⁸,
 E. Polcarpo², G.J. Pomery⁵⁴, S. Ponce⁴⁸, D. Popov^{6,48}, S. Popov⁴², S. Poslavskii⁴⁴,
 K. Prasanth³⁵, L. Promberger⁴⁸, C. Prouve⁴⁶, V. Pugatch⁵², H. Pullen⁶³, G. Punzi^{29,n}, H. Qi³,
 W. Qian⁶, J. Qin⁶, N. Qin³, R. Quagliani¹³, B. Quintana⁸, N.V. Raab¹⁸, R.I. Rabadan Trejo¹⁰,
 B. Rachwal³⁴, J.H. Rademacker⁵⁴, M. Rama²⁹, M. Ramos Pernas⁵⁶, M.S. Rangel²,
 F. Ratnikov^{42,82}, G. Raven³³, M. Reboud⁸, F. Redi⁴⁹, F. Reiss⁶², C. Remon Alepuz⁴⁷, Z. Ren³,
 V. Renaudin⁶³, R. Ribatti²⁹, S. Ricciardi⁵⁷, K. Rinnert⁶⁰, P. Robbe¹¹, G. Robertson⁵⁸,
 A.B. Rodrigues⁴⁹, E. Rodrigues⁶⁰, J.A. Rodriguez Lopez⁷⁴, A. Rollings⁶³, P. Roloff⁴⁸,
 V. Romanovskiy⁴⁴, M. Romero Lamas⁴⁶, A. Romero Vidal⁴⁶, J.D. Roth⁸⁶, M. Rotondo²³,
 M.S. Rudolph⁶⁸, T. Ruf⁴⁸, J. Ruiz Vidal⁴⁷, A. Ryzhikov⁸², J. Ryzka³⁴, J.J. Saborido Silva⁴⁶,
 N. Sagidova³⁸, N. Sahoo⁵⁶, B. Saitta^{27,e}, M. Salomoni⁴⁸, D. Sanchez Gonzalo⁴⁵,
 C. Sanchez Gras³², R. Santacesaria³⁰, C. Santamarina Rios⁴⁶, M. Santimaria²³,
 E. Santovetti^{31,p}, D. Saranin⁸³, G. Sarpis⁵⁹, M. Sarpis⁷⁵, A. Sarti³⁰, C. Satriano^{30,o}, A. Satta³¹,
 M. Saur¹⁵, D. Savrina^{41,40}, H. Sazak⁹, L.G. Scantlebury Smead⁶³, A. Scarabotto¹³, S. Schael¹⁴,
 M. Schiller⁵⁹, H. Schindler⁴⁸, M. Schmelling¹⁶, B. Schmidt⁴⁸, O. Schneider⁴⁹, A. Schopper⁴⁸,
 M. Schubiger³², S. Schulte⁴⁹, M.H. Schune¹¹, R. Schwemmer⁴⁸, B. Sciascia²³, S. Sellam⁴⁶,
 A. Semennikov⁴¹, M. Senghi Soares³³, A. Sergi²⁴, N. Serra⁵⁰, L. Sestini²⁸, A. Seuthe¹⁵,
 P. Seyfert⁴⁸, Y. Shang⁵, D.M. Shangase⁸⁶, M. Shapkin⁴⁴, I. Shchemerov⁸³, L. Shchutska⁴⁹,
 T. Shears⁶⁰, L. Shekhtman^{43,v}, Z. Shen⁵, V. Shevchenko⁸¹, E.B. Shields^{26,j}, E. Shmanin⁸³,
 J.D. Shupperd⁶⁸, B.G. Siddi²¹, R. Silva Coutinho⁵⁰, G. Simi²⁸, S. Simone^{19,c}, N. Skidmore⁶²,
 T. Skwarnicki⁶⁸, M.W. Slater⁵³, I. Slazyk^{21,f}, J.C. Smallwood⁶³, J.G. Smeaton⁵⁵,
 A. Smetkina⁴¹, E. Smith¹⁴, M. Smith⁶¹, A. Snoch³², M. Soares²⁰, L. Soares Lavra⁹,
 M.D. Sokoloff⁶⁵, F.J.P. Soler⁵⁹, A. Solovev³⁸, I. Solovyev³⁸, F.L. Souza De Almeida²,
 B. Souza De Paula², B. Spaan¹⁵, E. Spadaro Norella^{25,i}, P. Spradlin⁵⁹, F. Stagni⁴⁸, M. Stahl⁶⁵,
 S. Stahl⁴⁸, P. Steffko⁴⁹, O. Steinkamp^{50,83}, O. Stenyakin⁴⁴, H. Stevens¹⁵, S. Stone⁶⁸,
 M.E. Stramaglia⁴⁹, M. Straticiu³⁷, D. Strelakina⁸³, F. Suljik⁶³, J. Sun²⁷, L. Sun⁷³, Y. Sun⁶⁶,
 P. Svihra⁶², P.N. Swallow⁵³, K. Swientek³⁴, A. Szabelski³⁶, T. Szumlak³⁴, M. Szymanski⁴⁸,
 S. Taneja⁶², A.R. Tanner⁵⁴, A. Terentev⁸³, F. Teubert⁴⁸, E. Thomas⁴⁸, K.A. Thomson⁶⁰,
 V. Tisserand⁹, S. T’Jampens⁸, M. Tobin⁴, L. Tomassetti^{21,f}, D. Torres Machado¹, D.Y. Tou¹³,
 M.T. Tran⁴⁹, E. Trifonova⁸³, C. Trippel⁴⁹, G. Tuci^{29,n}, A. Tully⁴⁹, N. Tuning^{32,48}, A. Ukleja³⁶,
 D.J. Unverzagt¹⁷, E. Ursov⁸³, A. Usachov³², A. Ustyuzhanin^{42,82}, U. Uwer¹⁷, A. Vagner⁸⁴,
 V. Vagnoni²⁰, A. Valassi⁴⁸, G. Valenti²⁰, N. Valls Canudas⁸⁵, M. van Beuzekom³²,
 M. Van Dijk⁴⁹, E. van Herwijnen⁸³, C.B. Van Hulse¹⁸, M. van Veghel⁷⁹, R. Vazquez Gomez⁴⁶,
 P. Vazquez Regueiro⁴⁶, C. Vázquez Sierra⁴⁸, S. Vecchi²¹, J.J. Velthuis⁵⁴, M. Veltri^{22,r},
 A. Venkateswaran⁶⁸, M. Veronesi³², M. Vesterinen⁵⁶, D. Vieira⁶⁵, M. Vieites Diaz⁴⁹,

H. Viemann⁷⁶, X. Vilasis-Cardona⁸⁵, E. Vilella Figueras⁶⁰, A. Villa²⁰, P. Vincent¹³,
D. Vom Bruch¹⁰, A. Vorobyev³⁸, V. Vorobyev^{43,v}, N. Voropaev³⁸, K. Vos⁸⁰, R. Waldi¹⁷,
J. Walsh²⁹, C. Wang¹⁷, J. Wang⁵, J. Wang⁴, J. Wang³, J. Wang⁷³, M. Wang³, R. Wang⁵⁴,
Y. Wang⁷, Z. Wang⁵⁰, Z. Wang³, H.M. Wark⁶⁰, N.K. Watson⁵³, S.G. Weber¹³, D. Websdale⁶¹,
C. Weisser⁶⁴, B.D.C. Westhenry⁵⁴, D.J. White⁶², M. Whitehead⁵⁴, D. Wiedner¹⁵,
G. Wilkinson⁶³, M. Wilkinson⁶⁸, I. Williams⁵⁵, M. Williams⁶⁴, M.R.J. Williams⁵⁸,
F.F. Wilson⁵⁷, W. Wislicki³⁶, M. Witek³⁵, L. Witola¹⁷, G. Wormser¹¹, S.A. Wotton⁵⁵, H. Wu⁶⁸,
K. Wyllie⁴⁸, Z. Xiang⁶, D. Xiao⁷, Y. Xie⁷, A. Xu⁵, J. Xu⁶, L. Xu³, M. Xu⁷, Q. Xu⁶, Z. Xu⁵,
Z. Xu⁶, D. Yang³, S. Yang⁶, Y. Yang⁶, Z. Yang³, Z. Yang⁶⁶, Y. Yao⁶⁸, L.E. Yeomans⁶⁰, H. Yin⁷,
J. Yu⁷¹, X. Yuan⁶⁸, O. Yushchenko⁴⁴, E. Zaffaroni⁴⁹, M. Zavertyaev^{16,u}, M. Zdybal³⁵,
O. Zenaiev⁴⁸, M. Zeng³, D. Zhang⁷, L. Zhang³, S. Zhang⁵, Y. Zhang⁵, Y. Zhang⁶³,
A. Zharkova⁸³, A. Zhelezov¹⁷, Y. Zheng⁶, X. Zhou⁶, Y. Zhou⁶, X. Zhu³, Z. Zhu⁶, V. Zhukov^{14,40},
J.B. Zonneveld⁵⁸, Q. Zou⁴, S. Zucchelli^{20,d}, D. Zuliani²⁸, G. Zunica⁶².

¹Centro Brasileiro de Pesquisas Físicas (CBPF), Rio de Janeiro, Brazil

²Universidade Federal do Rio de Janeiro (UFRJ), Rio de Janeiro, Brazil

³Center for High Energy Physics, Tsinghua University, Beijing, China

⁴Institute Of High Energy Physics (IHEP), Beijing, China

⁵School of Physics State Key Laboratory of Nuclear Physics and Technology, Peking University, Beijing, China

⁶University of Chinese Academy of Sciences, Beijing, China

⁷Institute of Particle Physics, Central China Normal University, Wuhan, Hubei, China

⁸Univ. Savoie Mont Blanc, CNRS, IN2P3-LAPP, Annecy, France

⁹Université Clermont Auvergne, CNRS/IN2P3, LPC, Clermont-Ferrand, France

¹⁰Aix Marseille Univ, CNRS/IN2P3, CPPM, Marseille, France

¹¹Université Paris-Saclay, CNRS/IN2P3, IJCLab, Orsay, France

¹²Laboratoire Leprince-Ringuet, CNRS/IN2P3, Ecole Polytechnique, Institut Polytechnique de Paris, Palaiseau, France

¹³LPNHE, Sorbonne Université, Paris Diderot Sorbonne Paris Cité, CNRS/IN2P3, Paris, France

¹⁴I. Physikalisches Institut, RWTH Aachen University, Aachen, Germany

¹⁵Fakultät Physik, Technische Universität Dortmund, Dortmund, Germany

¹⁶Max-Planck-Institut für Kernphysik (MPIK), Heidelberg, Germany

¹⁷Physikalisches Institut, Ruprecht-Karls-Universität Heidelberg, Heidelberg, Germany

¹⁸School of Physics, University College Dublin, Dublin, Ireland

¹⁹INFN Sezione di Bari, Bari, Italy

²⁰INFN Sezione di Bologna, Bologna, Italy

²¹INFN Sezione di Ferrara, Ferrara, Italy

²²INFN Sezione di Firenze, Firenze, Italy

²³INFN Laboratori Nazionali di Frascati, Frascati, Italy

²⁴INFN Sezione di Genova, Genova, Italy

²⁵INFN Sezione di Milano, Milano, Italy

²⁶INFN Sezione di Milano-Bicocca, Milano, Italy

²⁷INFN Sezione di Cagliari, Monserrato, Italy

²⁸Università degli Studi di Padova, Università e INFN, Padova, Padova, Italy

²⁹INFN Sezione di Pisa, Pisa, Italy

³⁰INFN Sezione di Roma La Sapienza, Roma, Italy

³¹INFN Sezione di Roma Tor Vergata, Roma, Italy

³²Nikhef National Institute for Subatomic Physics, Amsterdam, Netherlands

³³Nikhef National Institute for Subatomic Physics and VU University Amsterdam, Amsterdam, Netherlands

³⁴AGH - University of Science and Technology, Faculty of Physics and Applied Computer Science, Kraków, Poland

³⁵Henryk Niewodniczanski Institute of Nuclear Physics Polish Academy of Sciences, Kraków, Poland

³⁶National Center for Nuclear Research (NCBJ), Warsaw, Poland

³⁷Horia Hulubei National Institute of Physics and Nuclear Engineering, Bucharest-Magurele, Romania

- ³⁸ Petersburg Nuclear Physics Institute NRC Kurchatov Institute (PNPI NRC KI), Gatchina, Russia
- ³⁹ Institute for Nuclear Research of the Russian Academy of Sciences (INR RAS), Moscow, Russia
- ⁴⁰ Institute of Nuclear Physics, Moscow State University (SINP MSU), Moscow, Russia
- ⁴¹ Institute of Theoretical and Experimental Physics NRC Kurchatov Institute (ITEP NRC KI), Moscow, Russia
- ⁴² Yandex School of Data Analysis, Moscow, Russia
- ⁴³ Budker Institute of Nuclear Physics (SB RAS), Novosibirsk, Russia
- ⁴⁴ Institute for High Energy Physics NRC Kurchatov Institute (IHEP NRC KI), Protvino, Russia, Protvino, Russia
- ⁴⁵ ICCUB, Universitat de Barcelona, Barcelona, Spain
- ⁴⁶ Instituto Galego de Física de Altas Enerxías (IGFAE), Universidade de Santiago de Compostela, Santiago de Compostela, Spain
- ⁴⁷ Instituto de Física Corpuscular, Centro Mixto Universidad de Valencia - CSIC, Valencia, Spain
- ⁴⁸ European Organization for Nuclear Research (CERN), Geneva, Switzerland
- ⁴⁹ Institute of Physics, Ecole Polytechnique Fédérale de Lausanne (EPFL), Lausanne, Switzerland
- ⁵⁰ Physik-Institut, Universität Zürich, Zürich, Switzerland
- ⁵¹ NSC Kharkiv Institute of Physics and Technology (NSC KIPT), Kharkiv, Ukraine
- ⁵² Institute for Nuclear Research of the National Academy of Sciences (KINR), Kyiv, Ukraine
- ⁵³ University of Birmingham, Birmingham, United Kingdom
- ⁵⁴ H.H. Wills Physics Laboratory, University of Bristol, Bristol, United Kingdom
- ⁵⁵ Cavendish Laboratory, University of Cambridge, Cambridge, United Kingdom
- ⁵⁶ Department of Physics, University of Warwick, Coventry, United Kingdom
- ⁵⁷ STFC Rutherford Appleton Laboratory, Didcot, United Kingdom
- ⁵⁸ School of Physics and Astronomy, University of Edinburgh, Edinburgh, United Kingdom
- ⁵⁹ School of Physics and Astronomy, University of Glasgow, Glasgow, United Kingdom
- ⁶⁰ Oliver Lodge Laboratory, University of Liverpool, Liverpool, United Kingdom
- ⁶¹ Imperial College London, London, United Kingdom
- ⁶² Department of Physics and Astronomy, University of Manchester, Manchester, United Kingdom
- ⁶³ Department of Physics, University of Oxford, Oxford, United Kingdom
- ⁶⁴ Massachusetts Institute of Technology, Cambridge, MA, United States
- ⁶⁵ University of Cincinnati, Cincinnati, OH, United States
- ⁶⁶ University of Maryland, College Park, MD, United States
- ⁶⁷ Los Alamos National Laboratory (LANL), Los Alamos, United States
- ⁶⁸ Syracuse University, Syracuse, NY, United States
- ⁶⁹ School of Physics and Astronomy, Monash University, Melbourne, Australia, associated to ⁵⁶
- ⁷⁰ Pontifícia Universidade Católica do Rio de Janeiro (PUC-Rio), Rio de Janeiro, Brazil, associated to ²
- ⁷¹ Physics and Micro Electronic College, Hunan University, Changsha City, China, associated to ⁷
- ⁷² Guangdong Provincial Key Laboratory of Nuclear Science, Institute of Quantum Matter, South China Normal University, Guangzhou, China, associated to ³
- ⁷³ School of Physics and Technology, Wuhan University, Wuhan, China, associated to ³
- ⁷⁴ Departamento de Física, Universidad Nacional de Colombia, Bogota, Colombia, associated to ¹³
- ⁷⁵ Universität Bonn - Helmholtz-Institut für Strahlen und Kernphysik, Bonn, Germany, associated to ¹⁷
- ⁷⁶ Institut für Physik, Universität Rostock, Rostock, Germany, associated to ¹⁷
- ⁷⁷ Eotvos Lorand University, Budapest, Hungary, associated to ⁴⁸
- ⁷⁸ INFN Sezione di Perugia, Perugia, Italy, associated to ²¹
- ⁷⁹ Van Swinderen Institute, University of Groningen, Groningen, Netherlands, associated to ³²
- ⁸⁰ Universiteit Maastricht, Maastricht, Netherlands, associated to ³²
- ⁸¹ National Research Centre Kurchatov Institute, Moscow, Russia, associated to ⁴¹
- ⁸² National Research University Higher School of Economics, Moscow, Russia, associated to ⁴²
- ⁸³ National University of Science and Technology "MISIS", Moscow, Russia, associated to ⁴¹
- ⁸⁴ National Research Tomsk Polytechnic University, Tomsk, Russia, associated to ⁴¹
- ⁸⁵ DS4DS, La Salle, Universitat Ramon Llull, Barcelona, Spain, associated to ⁴⁵
- ⁸⁶ University of Michigan, Ann Arbor, United States, associated to ⁶⁸

^a Universidade Federal do Triângulo Mineiro (UFTM), Uberaba-MG, Brazil

^b Hangzhou Institute for Advanced Study, UCAS, Hangzhou, China

^c Università di Bari, Bari, Italy

- ^d *Università di Bologna, Bologna, Italy*
^e *Università di Cagliari, Cagliari, Italy*
^f *Università di Ferrara, Ferrara, Italy*
^g *Università di Firenze, Firenze, Italy*
^h *Università di Genova, Genova, Italy*
ⁱ *Università degli Studi di Milano, Milano, Italy*
^j *Università di Milano Bicocca, Milano, Italy*
^k *Università di Modena e Reggio Emilia, Modena, Italy*
^l *Università di Padova, Padova, Italy*
^m *Scuola Normale Superiore, Pisa, Italy*
ⁿ *Università di Pisa, Pisa, Italy*
^o *Università della Basilicata, Potenza, Italy*
^p *Università di Roma Tor Vergata, Roma, Italy*
^q *Università di Siena, Siena, Italy*
^r *Università di Urbino, Urbino, Italy*
^s *MSU - Iligan Institute of Technology (MSU-IIT), Iligan, Philippines*
^t *AGH - University of Science and Technology, Faculty of Computer Science, Electronics and Telecommunications, Kraków, Poland*
^u *P.N. Lebedev Physical Institute, Russian Academy of Science (LPI RAS), Moscow, Russia*
^v *Novosibirsk State University, Novosibirsk, Russia*
^w *Department of Physics and Astronomy, Uppsala University, Uppsala, Sweden*
^x *Hanoi University of Science, Hanoi, Vietnam*